Acta Cryst. (1996). B52, 610–615

Antiferroelectric Modulations in Sb_2WO_6 and Sb_2MoO_6

CHRISTOPHER D. LING,* RAY L. WITHERS, A. DAVID RAE, SIEGBERT SCHMID AND JOHN G. THOMPSON

Research School of Chemistry, Australian National University, Canberra ACT 0200, Australia. E-mail: ling@rsc.anu.edu.au

(*Received 27 November 1995; accepted 15 March 1996*)

Abstract

The structure of Sb_2WO_6 [M_r = 523.4, triclinic, $F\bar{1}$, a = 11.132 (1), b = 9.896 (4), c = 18.482 (7) Å, α = 90.20 (4), β = 96.87 (8), γ = 90.21 (5)°, D_x = 6.88 g cm^{-3}, Z = 16, Mo $K\alpha$, λ = 0.7107 Å, μ = 338.5 cm^{-1}, $F(000)$ = 3536] has been refined as an enlarged 2**a** × 2**b** × 2**c** F-centred superstructure of the previously reported structure [Castro, Millan, Enjalbert, Snoeck & Galy (1994). *Mat. Res. Bull.* **29**, 871–879] refined in the space group $P1$. The re-refinement follows the observation, initially by TEM, of satellite reflections at $\mathbf{G} \pm \frac{1}{2}(111)^*$, where **G** represents a reflection of the $P1$ reciprocal lattice. A final value of 0.040 for $R_1 = \sum_h ||F_{obs}(\mathbf{h})| - |F_{calc}(\mathbf{h})||/\sum_h |F_{obs}(\mathbf{h})|$ was obtained for 3316 merged reflections with $I(\mathbf{h}) > 3\sigma[I(\mathbf{h})]$, compared with R_1 = 0.12 for the previous refinement. The refined structure is described in terms of an antiferroelectric modulation of a $P12_1/a1$ underlying parent structure in the original setting. Twinning of the crystal was successfully modelled in the refinement. Synthesis of the previously unknown phase Sb_2MoO_6 [M_r = 435.5, triclinic, $F\bar{1}$, a = 10.758 (1), b = 9.673 (2), c = 17.57 (1) Å, α = 90.00 (5), β = 96.98 (3), γ = 90.05 (2)°, Z = 16, D_x = 4.97 g cm^{-3}] is also reported, along with evidence for its isostructuralism with Sb_2WO_6.

1. Introduction

The existence and crystal structure of Sb_2WO_6 has very recently been reported and described as an antimony-based analogue to the n = 1 members of the bismuth-based Aurivillius family of layered oxide structures (Castro, Millan, Enjalbert, Snoeck & Galy, 1994). Aurivillius phases consist of ordered intergrowths between single layer slabs of α-PbO ($Bi_2O_2^{2+}$) and slabs n layers thick of perovskite [$A_{n-1}B_nO_{3n+1}^{2+}$ (Aurivillius, 1949)]. Sb_2WO_6 was described as an ordered intergrowth between α-Sb_2O_3 ($Sb_2O_2^{2+}$) and perovskite (WO_4^{2-}), *i.e.* n = 1, B = W. The triclinic unit cell reported was set in an orientation analogous to those used for Aurivillius phases, although Aurivillius phases generally have monoclinic cells derived from tetragonal parent structures by symmetry-lowering modulations (Withers, Thompson & Rae, 1991).

The previously reported triclinic unit cell for Sb_2WO_6 contained two angles (α = 90.05, γ = 90.20°) very close to 90°, making the cell pseudo-monoclinic. In addition, the reported fractional atomic coordinates refined by Castro *et al.* (1994) in the space group $P1$ very nearly obeyed space-group symmetry $P12_1/a1$. This suggested the existence of an underlying parent substructure of exact monoclinic symmetry, which is somehow modulated to produce the final resultant structure. Considering the poor residual obtained for the previous structure refinement (R = 0.12), it was thought that the symmetry-lowering modulation from this parent structure may have been treated incorrectly. [Castro *et al.* (1994) recognized the possibility of problems arising from the existence of twinning and hence chose to use reflections associated with a single twin component. It was suggested that the poor residual may have been a result of such problems.] Calculation of atomic valences (AV's) by the bond length–bond valence method (Brese & O'Keeffe, 1991) indicated chemical problems with the previously reported structure, *e.g.* W(2) had an AV of 6.57 and was bonded to O(2) and O(4) with AV's of 2.69 and 1.39, respectively. The reported position of this W atom, therefore, appeared improbable. This further supported the hypothesis of an incorrectly treated modulation.

Given the previously demonstrated usefulness of a modulation wave approach in describing and refining the structures of Aurivillius phases (Rae, Thompson & Withers, 1991, 1992; Thompson, Rae, Withers & Craig, 1991), it was decided to re-examine the reported unit cell and space-group symmetry of Sb_2WO_6 *via* an electron diffraction study. Electron diffraction has a proven ability to observe weak features of reciprocal space often missed *via* conventional X-ray diffraction procedures and, in this case, led to the observation of previously unobserved $\mathbf{G} \pm \frac{1}{2}(111)^*$ satellite reflections. It was, therefore, decided to re-refine the structure from X-ray data using a modulation wave approach. An investigation was also made into the existence of a potentially isomorphous phase Sb_2MoO_6, in order to corroborate any findings about Sb_2WO_6. Such a phase was found to exist and was investigated by X-ray powder diffraction and electron diffraction. Crystals suitable for X-ray study could not, however, be grown.

2. Experimental

Experimental details are summarized in Table 1. Crystals of Sb_2WO_6 were grown by the method of Castro *et al.* (1994). A mixture of Sb_2O_3 (Aldrich 99.99%) and WO_3

Table 1. *Experimental details*

Crystal data	
Chemical formula	WSb_2O_6
Chemical formula weight	523.4
Cell setting	Triclinic
Space group	$F\bar{1}$
a (Å)	11.132 (1)
b (Å)	9.896 (4)
c (Å)	18.482 (7)
α (°)	90.20 (4)
β (°)	96.87 (8)
γ (°)	90.21 (5)
V (Å^3)	2021 (1)
Z	16
D_x (Mg m^{-3})	6.88
Radiation type	Mo $K\alpha$
Wavelength (Å)	0.7107
No. of reflections for cell parameters	25
θ range (°)	6–14
μ (mm^{-1})	33.85
Temperature (K)	295
Crystal form	Plate
Crystal size (mm)	0.09 × 0.08 × 0.003
Crystal color	Yellow
Data collection	
Diffractometer	Philips PW1100
Data collection method	ω–2θ
Absorption correction	Weighted Gaussian grid
T_{min}	0.1
T_{max}	0.9
No. of measured reflections	8868
No. of independent reflections	4434
No. of observed reflections	3316
Criterion for observed reflections	$I > 3\sigma(I)$
R_{int}	0.039
θ_{max} (°)	25
Range of h, k, l	$-17 \rightarrow h \rightarrow 17$ $-15 \rightarrow k \rightarrow 15$ $-28 \rightarrow l \rightarrow 28$
No. of standard reflections	3
Frequency of standard reflections (min)	120
Refinement	
Refinement on	F
R	0.040
wR	0.053
S	1.19
No. of reflections used in refinement	3316
No. of parameters used	93
Weighting scheme	Weighting scheme includes a random 3% error in F obtained from merge statistics
$(\Delta/\sigma)_{max}$	0.4
$\Delta\rho_{max}$ (e Å^{-3})	1.2
$\Delta\rho_{min}$ (e Å^{-3})	−1.5
Extinction method	Coppens & Hamilton (1970)
Extinction coefficient	Type I: $z'_{11} = z'_{33} = 0.0006$ (3); $z'_{22} = 0.028$ (7)
Source of atomic scattering factors	*International Tables for Crystallography* (1992, Vol. C)

(Koch-Lite 99.9%) was heated with the mole ratio 4:1 in a sealed, evacuated silica ampoule to 1073 K for 24 h, then steadily cooled to 673 K over 80 h. Small, transparent yellow, plate-like crystals were formed on the surface of the specimen. The X-ray powder diffraction pattern of ground crystals matched that reported by Castro *et al.* (1994) for Sb_2WO_6.

The crystal of Sb_2WO_6 chosen for X-ray data collection was selected using a transmission optical microscope with crossed polarizers and was free of 90° domain walls. The cut crystal was a plate with the thin dimension corresponding to the crystallographic **c*** axis of the $F\bar{1}$ cell. The crystal was found to be twinned with respect to a plane perpendicular to **c***, reflections of the minor component being related to those of the major component by the rule $h' = h$, $k' = k$, $l' = -l - 2ca^*\sin\alpha \sin\beta^* \cos\beta^* h - 2cb^*\sin\beta \sin\alpha^* \cos\alpha^* k = -1 - 0.40045h - 0.01497k$. Overlap of twin reflections was accounted for using the method of Rae (1987), the minor twin volume being refined to 4.7 (2)% of the total volume. Only reflections with $h = 5n$ are overlapped. The absorption correction, μ(Mo $K\alpha$) = 338.5 cm^{-1}, used distances to the seven faces from an internal origin of (0,11,$\bar{2}$) 0.0309, ($\bar{1}\bar{1}$1) 0.0295, (11$\bar{1}$) 0.0486, (00$\bar{1}$) 0.0015 (2), (001) 0.0015 (2), (11,$\bar{1}$,$\bar{9}$) 0.0612 and ($\bar{2}$21) 0.0627 mm. The numerical correction used a 12 × 12 × 12 grid with grid layers perpendicular to **c***. The thin dimension was optimized as part of the refinement.

A full sphere of F-centred Mo $K\alpha$ monochromator data with $1.5 < \theta < 35°$ was collected on a Philips PW1100 diffractometer in $\omega/2\theta$ scan mode with a scan speed of 1.5° min^{-1} and an ω-scan width of (1.0 + 0.35tan θ). The dimensions of the $F\bar{1}$ unit cell of Sb_2WO_6 were calculated from 25 reflections; a = 11.132 (1), b = 9.896 (4), c = 18.482 (7) Å, α = 90.20 (4), β = 96.87 (8), γ = 90.21 (5)°, D_x = 6.88 g cm^{-3}. Scattering curves, atomic absorption coefficients and anomalous-dispersion coefficients were taken from *International Tables for X-ray Crystallography* (1992, Vol. C).

A powder of Sb_2MoO_6 was grown by solid-state reaction of a mixture of Sb_2O_3 (Aldrich 99.99%) and MoO_3 (Halewood 99.999%) with mole ratio 1.1:1, in a sealed platinum tube, heated to 948 K for 100 h and then quenched in air. The X-ray powder diffraction pattern of the orange powder was very similar to that of Sb_2WO_6. Dimensions of the $F\bar{1}$ unit cell of Sb_2MoO_6 were obtained by X-ray powder diffraction using a Guinier–Hägg camera with Cu $K\alpha_1$ radiation and Si as an internal standard (NBS standard number 640); a = 10.758 (1), b = 9.673 (2), c = 17.57 (1) Å, α = 90.00 (5), β = 96.98 (3), γ = 90.05 (2)°, Z = 16, D_x = 4.97 g cm^{-3}.

3. Results

3.1. *Electron diffraction*

Single crystal grains of Sb_2WO_6 and Sb_2MoO_6 were studied by electron diffraction using Jeol 100CX and Philips EM430 transmission electron microscopes (TEM's). Microdiffraction patterns of Sb_2MoO_6 were found to be entirely analogous to those of Sb_2WO_6, suggesting that the former, previously unreported, phase is entirely isostructural with the latter.

Table 2. *Allowed irreducible representations associated with the* $\mathbf{q} = \frac{1}{2}(111)^*$ *primary modulation wavevector*

	$\{E\|\mathbf{0}\}$	$\{E\|\mathbf{b}\}$	$\{\sigma_y\|\frac{1}{2}(\mathbf{a}+\mathbf{b})\}$	$\{\sigma_y\|\frac{1}{2}(-\mathbf{a}+\mathbf{b})\}$	$\{i\|\mathbf{0}\}$	$\{i\|\mathbf{b}\}$	$\{C_{2y}\|\frac{1}{2}(\mathbf{a}+\mathbf{b})\}$	$\{C_{2y}\|\frac{1}{2}(-\mathbf{a}+\mathbf{b})\}$
R_2	1	−1	$-i$	i	−1	1	i	$-i$
R_4	1	−1	i	$-i$	−1	1	$-i$	i
R_6	1	−1	i	$-i$	1	−1	i	$-i$
R_8	1	−1	$-i$	i	1	−1	$-i$	i

Microdiffraction patterns taken down the (*a*) [001], (*b*) [010] and (*c*) [011] zone axes of the previously reported cell are shown in Fig. 1. The [001] zone axis pattern shows the reciprocal cell parameters reported by Castro *et al.* (1994) in the zeroth-order Laue zone (ZOLZ), with no extinction conditions. Reflections in the first-order Laue zone (FOLZ), however, occur at a height of $c^*/2$ in terms of that cell. Moreover, projection of the FOLZ onto the ZOLZ clearly shows reflections of the former to be at ($a^*/2$, $b^*/2$) with respect to the latter. The FOLZ is, therefore, exhibiting satellite reflections at $\mathbf{G} \pm \frac{1}{2}(111)^*$, where **G** represents reflections belonging to the reciprocal lattice published by Castro *et al.* (1994). This is confirmed by the existence of $\mathbf{G} \pm \frac{1}{2}(111)^*$-type satellite reflections in the ZOLZ of the [011] microdiffraction pattern shown in Fig. 1(*c*). Note the weakness of the *h*0*l*, *h* = odd, reflections in Fig. 1(*b*). The weakness of these observed reflections is consistent with the underlying $P12_1/a1$ parent space-group symmetry.

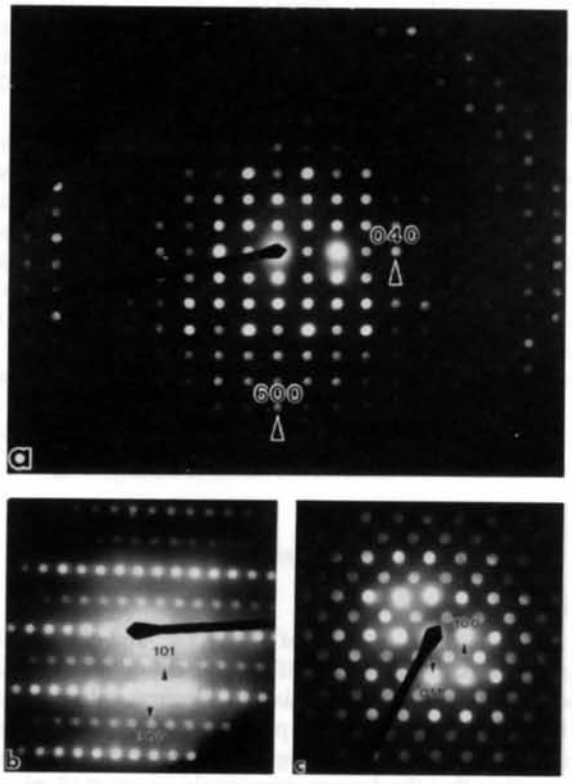

Fig. 1. Microdiffraction patterns of Sb_2WO_6 taken down the (*a*) [001], (*b*) [010] and (*c*) [011] zone axes.

The simplest interpretation of these additional $\mathbf{G} \pm \frac{1}{2}(111)^*$ satellite reflections is that Sb_2WO_6 has a $2\mathbf{a} \times 2\mathbf{b} \times 2\mathbf{c}$ face-centred supercell of the unit cell reported by Castro *et al.* (1994). No extinction conditions were observed for the cell in this setting other than those due to *F*-centring.

3.2. *Group theoretical considerations*

The *F*-centred unit cell of Sb_2WO_6 is superficially related to the cell reported by Castro *et al.* (1994) by a doubling of all axes, in accordance with the additional $\mathbf{G} \pm \frac{1}{2}(111)^*$ reflection data observed. The resultant structure itself can be described in terms of an underlying $P12_1/a1$ parent structure (derivable from the previously reported structure of Sb_2WO_6) plus displacive modulations thereof characterized by the primary modulation wavevector $\mathbf{q} = \frac{1}{2}(111)^*$ and the second harmonic modulation wavevector $\mathbf{q} = 0$ (responsible for the weakly observed *h*0*l*, *h* = odd, reflections in Fig. 1*b*).

Given a $P12_1/a1$ parent structure, Table 2 lists the four possible irreducible representations associated with the primary modulation wavevector $\mathbf{q} = \frac{1}{2}(111)^*$ (for details, see Bradley & Cracknell, 1972). Time-reversal symmetry links the R_2, R_4 and R_6, R_8 irreducible representations into pairs so that there are only two distinct displacive mode symmetries possible. Note that neither can give rise to a resultant structure of monoclinic space-group symmetry. Only parent symmetry operations with a character of +1 in Table 2 are preserved in the resultant structure. Both R_2, R_4 and R_6, R_8 displacive modes individually give rise to resultant $F\bar{1}$ space-group symmetry. (If modes of both symmetry types were simultaneously present, the resultant space-group symmetry would be $F1$.) In the former case, the resultant inversion centre is located at $\frac{1}{2}\mathbf{b}$ with respect to the origin of Castro *et al.* (1994), *i.e.* midway between W atoms, whereas the resultant inversion centre in the case of an R_6, R_8 displacive mode is located at the origin of Castro *et al.* (1994), *i.e.* on the W atoms. The W atoms are, therefore, only allowed to move for a displacive mode of R_2, R_4 symmetry. WO_6 octahedral rotations are, therefore, associated with modes of R_6, R_8 symmetry, whereas 'ferroelectric' shifts of the W atoms away from the centre of their coordinating octahedra of oxygen ions can only be associated with modes of R_2, R_4 symmetry.

The final refined structure (see below) unambiguously requires the $\mathbf{q} = \frac{1}{2}(111)^*$ displacive modulation to be associated with the latter type of distortion and thus requires the deviation of the resultant structure from

Table 3. *Fractional atomic coordinates*

$U_{eq} = (1/3)\sum_i\sum_j U_{ij}a_i^*a_j^*\mathbf{a}_i.\mathbf{a}_j$.

	x	*y*	*z*
W1	−0.02139 (4)	0.50291 (4)	0.25026 (2)
W2	0.24462 (4)	0.27221 (4)	0.24436 (2)
Sb1	0.18111 (7)	0.01967 (7)	0.08258 (4)
Sb2	0.43404 (7)	0.72697 (7)	0.08312 (2)
Sb3	0.18143 (7)	0.52925 (7)	0.08447 (4)
Sb4	0.43068 (7)	0.22228 (7)	0.08585 (4)
O1	0.0698 (7)	0.1548 (8)	0.0326 (5)
O2	0.3177 (7)	0.5962 (8)	0.0309 (5)
O3	0.0667 (7)	0.6589 (8)	0.0320 (5)
O4	0.3189 (7)	0.0882 (8)	0.0332 (5)
O5	−0.0129 (8)	0.0726 (8)	0.1568 (5)
O6	0.2431 (7)	0.6825 (7)	0.1561 (5)
O7	−0.0025 (8)	0.5725 (8)	0.1564 (5)
O8	0.2423 (8)	0.1726 (8)	0.1574 (5)
O9	0.1048 (7)	0.3585 (7)	0.2194 (5)
O10	0.3537 (7)	0.3946 (7)	0.2199 (5)
O11	0.1045 (7)	0.8574 (7)	0.2210 (5)
O12	0.3528 (7)	0.8935 (7)	0.2200 (5)

the underlying $P12_1/a1$ parent structure to be described in terms of the condensation of an R_2, R_4 symmetry type, $\mathbf{q} = \frac{1}{2}(111)^*$ displacive modulation. The infinite wavelength strain wave accompanying this R_2, R_4, $\mathbf{q} = \frac{1}{2}(111)^*$ displacive modulation is then responsible for the very slight triclinic distortion of the original monoclinic parent unit cell.

3.3. *Structure refinement of Sb_2WO_6*

The non-standard *F*-centred setting of the unit cell, as defined above, was retained for the structure refinement. This allows the relationship between the modulated and parent structures to be most conveniently discussed. [Note that the standard, Niggli reduced, primitive cell is defined by $\mathbf{a}' = \frac{1}{2}(\mathbf{a} + \mathbf{b})$, $\mathbf{b}' = \frac{1}{2}(\mathbf{a} - \mathbf{b})$, $\mathbf{c}' = \frac{1}{2}(\mathbf{a} + \mathbf{c})$.] The above group theoretical considerations show that the only possible resultant space-group symmetries are $F1$ or $F\bar{1}$. The structure was refined in $F\bar{1}$. There was no indication of any necessity to lower the symmetry further.

From 4434 merged reflections, the 3316 with $I(\mathbf{h}) > 3\sigma(I(\mathbf{h}))$ were used in refinement. Final values of $R_1 = \sum_\mathbf{h}||F_{obs}(\mathbf{h})| - |F_{calc}(\mathbf{h})||/\sum_\mathbf{h}|F_{obs}(\mathbf{h})|$ of 0.040 and $wR = [\sum_\mathbf{h} w_\mathbf{h}[|F_{obs}(\mathbf{h})| - |F_{calc}(\mathbf{h})|]2/\sum_\mathbf{h} w_\mathbf{h}|F_{obs}(\mathbf{h})|2]^{1/2}$ of 0.053 were obtained with a goodness-of-fit value of 1.19. The 3316 observed reflections were divided into four subsets, *viz.* 1394 parent reflections with $h \neq 5n$, 1244 modulating reflections with $h \neq 5n$, 374 parent reflections with $h = 5n$ and 305 modulating reflections with $h = 5n$. Respective values were 0.041, 0.040, 0.041, 0.041 for R_1 and 0.054, 0.051, 0.056, 0.049 for wR. To allow for the possibility of stacking faults, a second scale for reflections with h odd was considered but found to be unnecessary. The size of the W displacements caused the average value of $|F_{obs}(\mathbf{h})|^2$ for the observed reflections with h odd to be smaller by a factor of 0.46 compared with reflections with h even. Anisotropic extinction parameters with the type 1 parameterization of Coppens & Hamilton (1970) were used. Refinement used the program *RAELS*92 (Rae, 1992). The final refined values for the fractional coordinates of Sb_2WO_6 are given in Table 3, with anisotropic thermal parameters in Table 4.† [U_{ij} are defined relative to orthonormal axes parallel to **a**, $\mathbf{c}^* \times \mathbf{a}$ and $\mathbf{c}^*$, such that the mean-square thermal displacement $U_{eq} = (U_{11} + U_{22} + U_{33})/3$.] The parent $P2_1/a$ symmetry relates sets of four atoms in the final structure and thermal parameters within these sets were constrained to maintain this symmetry relationship. The W atoms were unconstrained. The uniformly good refinement statistics and the well behaved anisotropic thermal parameters of the O atoms are indicative of a correct refinement and this is substantiated by the calculated apparent valences (see Table 5). Major zone axis projections of the structure plotted by the program *CrystalMaker* (Palmer, 1994) are presented in Fig. 2.

Deviations of the real structure away from the $P12_1/a1$ parent structure associated with the R^2, R^2 symmetry, $\mathbf{q} = \frac{1}{2}(111)^*$ primary modulation may be identified by comparing the final fractional coordinates of sets of atoms given in Table 6.

Table 4. *U_{ij} thermal parameters for Sb_2WO_6 (10^{-3} Å^2)*

	U_{11}	U_{22}	U_{33}	U_{12}	U_{13}	U_{23}	U_{eq}
W(1)	6.1 (1)	4.4 (1)	6.2 (1)	0.7 (1)	−0.1 (1)	0.9 (1)	5.4 (1)
W(2)	7.6 (1)	2.4 (1)	6.1 (1)	0.2 (1)	−0.2 (1)	0.2 (1)	5.1 (1)
Sb(1)	10.2 (1)	7.2 (1)	9.7 (1)	0.1 (1)	−1.5 (1)	1.8 (1)	9.0 (1)
O(1)	10 (2)	14 (2)	11 (2)	5 (1)	2 (1)	3 (1)	12 (1)
O(5)	16 (2)	8 (1)	9 (2)	2 (1)	0 (1)	1 (1)	11 (1)
O(9)	12 (2)	6 (1)	11 (2)	1 (1)	−2 (1)	4 (1)	10 (1)

Atoms Sb(3), O(3), O(7) and O(11) were constrainted to have the same values as atoms Sb(1), O(1), O(5) and O(9), respectively. Atoms labelled Sb(2*N*) or O(2*N*) and atoms labelled Sb(2*N* − 1) or O(2*N* − 1) have the same values for U_{11}, U_{22}, U_{33} and U_{13}, but values for U_{12} and U_{23} switch signs.

Table 5. *Apparent valences of tungsten and oxygen in Sb_2WO_6 and in its $P12_1/a1$ parent structure*

	$F\bar{1}$ superstructure apparent valence	$P12_1/a1$ substructure apparent valence
Sb(1)	3.143	3.113
Sb(2)	3.135	3.113
Sb(3)	3.114	3.113
Sb(4)	3.126	3.113
W(1)	6.169	6.192
W(2)	6.153	6.192
O(1)	2.138	1.908
O(2)	2.162	1.908
O(3)	2.171	1.908
O(4)	2.180	1.908
O(5)	1.994	2.117
O(6)	2.030	2.117
O(7)	2.023	2.117
O(8)	1.988	2.117
O(9)	2.058	2.184
O(10)	1.986	2.184
P(11)	2.058	2.184
O(12)	2.051	2.184

† A list of structure factors has been deposited with the IUCr (Reference: JS0034). Copies may be obtained through The Managing Editor, International Union of Crystallography, 5 Abbey Square, Chester CH1 2HU, England.

Table 6. *Atom pairs in Sb_2WO_6 initially related by the parent structure lattice translation $\mathbf{b}_{parent} = \frac{1}{2}\mathbf{b}_{real}$*

In the absence of the $\mathbf{q} = \frac{1}{2}(111)^*$ modulation the relationship between the fractional coordinates of such atom pairs in the resultant structure should be $x, \frac{1}{2}+y, z$. The relating pairs of atoms in the space-group symmetry operation of the resultant structure are given. In the absence of the $\mathbf{q} = \frac{1}{2}(111)^*$ modulation the relationship between the fractional coordinates of pairs of atoms in adjacent rows of the table should be $\frac{1}{4}+x, \frac{1}{4}-y, z$.

Atom1	Atom 2	Relationship
W(1)	W(1)	$-x, \frac{1}{2}-y, \frac{1}{2}-z$
W(2)	W(2)	$\frac{1}{2}-x, 1-y, \frac{1}{2}-z$
Sb(1)	Sb(3)	
Sb(4)	Sb(2)	
O(1)	O(3)	
O(4)	O(2)	
O(5)	O(7)	
O(6)	O(8)	
O(9)	O(11)	
O(10)	O(12)	

Table 7. *Selected geometric parameters* (Å, °)

W1—O5^{i}	1.872 (8)	W2—O6^{ii}	1.881 (8)
W1—O7	1.903 (8)	W2—O8	1.879 (8)
W1—O9	2.131 (7)	W2—O9	1.790 (8)
W1—O10^{ii}	2.134 (7)	W2—O10	1.809 (7)
W1—O11^{iii}	1.781 (7)	W2—O11^{ii}	2.154 (8)
W1—O12^{iv}	1.800 (7)	W2—O12^{ii}	2.114 (7)
Sb1—O1	1.981 (8)	Sb2—O2	1.991 (8)
Sb1—O4	1.995 (8)	Sb2—O1^{vi}	2.002 (8)
Sb1—O8	2.102 (8)	Sb2—O5^{vi}	2.089 (8)
Sb1—O2^{v}	2.387 (8)	Sb2—O3^{vii}	2.411 (8)
Sb1—O5	2.746 (8)	Sb2—O6	2.686 (6)
Sb3—O3	1.985 (8)	Sb4—O4	1.986 (8)
Sb3—O2	2.020 (8)	Sb4—O3^{viii}	2.011 (8)
Sb3—O6	2.070 (8)	Sb4—O7^{viii}	2.059 (8)
Sb3—O4^{v}	2.461 (8)	Sb4—O1^{v}	2.507 (8)
Sb3—O7	2.608 (8)	Sb4—O8	2.657 (8)

Symmetry codes: (i) $-x, \frac{1}{2}-y, \frac{1}{2}-z$; (ii) $\frac{1}{2}-x, 1-y, \frac{1}{2}-z$; (iii) $-x, \frac{3}{2}-y, \frac{1}{2}-z$; (iv) $x-\frac{1}{2}, y-\frac{1}{2}, z$; (v) $\frac{1}{2}-x, \frac{1}{2}-y, -z$; (vi) $\frac{1}{2}+x, \frac{1}{2}+y, z$; (vii) $\frac{1}{2}-x, \frac{3}{2}-y, -z$; (viii) $\frac{1}{2}+x, y-\frac{1}{2}, z$.

Comparing the ideal parent relationship to the real coordinates (Table 3), it can readily be seen that none of the Sb and O atoms deviate significantly from their positions in the parent substructure. W atoms, however, do; W1 shifts primarily along **a** and W2 primarily along **b** by approximately 0.23 Å in each case. The relative magnitude of these W-atom shifts can be seen in Fig. 2, W atoms being the only ones not eclipsed in the major zone axis projections of the resultant structure. W-atom displacements away from the centre of their coordinating octahedra of oxygen ions represent the dominant distortion from the monoclinic parent substructure, hence the driving force for symmetry lowering.

The basic pattern of these W-atom shifts is antiferroelectric in nature and shown in Fig. 3, demonstrating the need for an enlarged cell relative to **a** and **b**. The **c** enlargement comes from inversion of this pattern of atomic shifts on adjacent layers along **c**. In order to investigate whether the driving force for these antiferroelectric displacements could be ascribed to optimization of AV requirements for atoms in the structure (Brown, 1978; Brese & O'Keefe, 1991), as is the case for the Aurivillius family of displacive ferroelectrics (Withers *et al.*, 1991), AV's were calculated for both the resultant structure and underlying substructure (Table 5) using the R_0 values given in Brese & O'Keeffe (1991). Calculation of AV's for tungsten and oxygen found that, indeed, very good values are obtained for the determined structure. However, moving W atoms to the centre of their coordinating octahedra of O atoms (*i.e.* to the parent substructure positions) did not make

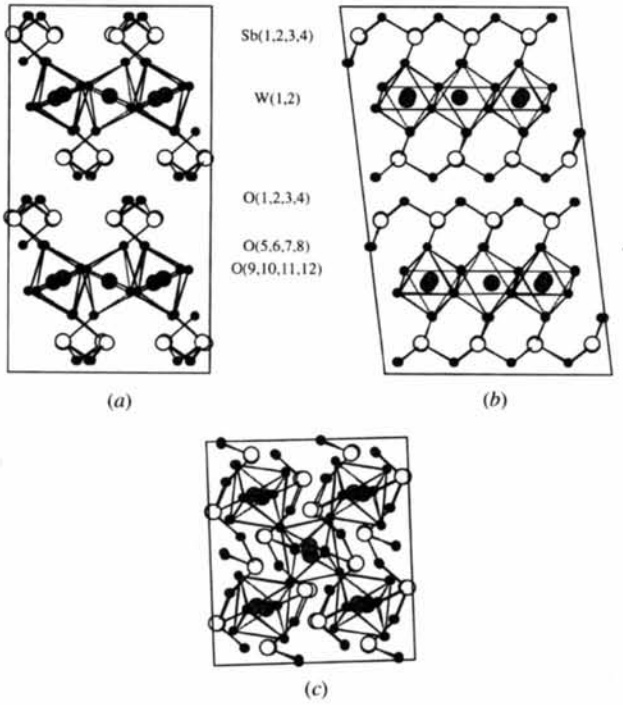

Fig. 2. (*a*) [100], (*b*) [010] and (*c*) [001] zone axis projections of Sb_2WO_6. Only complete WO_6 coordination octahedra are drawn.

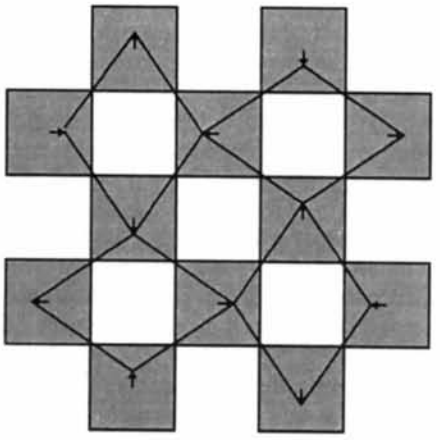

Fig. 3. The principal pattern of W-atom displacements from the parent substructure positions of Sb_2WO_6. Shifts are exaggerated by a factor of approximately four.

the AV's unreasonable (Table 5). Therefore, simple AV considerations allow, but do not explain the driving force behind, the observed symmetry lowering.

While not an explanation for the antiferroelectric pattern of W-atom shifts in the WO_4^{2-} portion of the Sb_2WO_6 structure, it is undoubtedly of significance that ideal WO_3 itself is reported to exhibit six distinct perovskite-related polymorphs and five displacive structural phase transitions in the range from 93 to 1173 K. The symmetry of these polymorphs ranges from tetragonal to orthorhombic to monoclinic to triclinic and back to monoclinic upon cooling (Salje, 1977). As for the WO_4^{2-} portion of the Sb_2WO_6 structure, it would appear that all these polymorphs are characterized by essentially regular, corner-connected WO_6 octahedra in which the W atoms are appreciably off-centre (Diehl, Brandt & Salje, 1978; Loopstra & Boldrini, 1966; Salje, 1977). A rather similar antiferroelectric pattern of tungsten movement to that observed in Sb_2WO_6 occurs in the room-temperature triclinic form of WO_3 [viewed on its (101) plane (Diehl *et al.*, 1978)]. The crystal chemistry underlying this phenomenon would appear to be an important problem in solid-state chemistry. A recent paper by Kunz & Brown (1995) has examined this problem.

The refined structure of Sb_2WO_6 reported in this paper may be described as ordered intergrowths of slabs of α-Sb_2O_3 ($Sb_2O_2^{2+}$) and triclinic WO_3 (WO_4^{2-}). Although a crystal of Sb_2MoO_6 suitable for X-ray study could not be obtained, the very close similarity of its electron and X-ray powder diffraction patterns to those of Sb_2WO_6 leaves us confident that the two phases are isostructural and that the $\mathbf{q} = \frac{1}{2}(111)^*$ modulation in this phase is also due to antiferroelectric shifts of the Mo atoms away from the centre of their oxygen coordination octahedra.

References

Aurivillius, B. (1949). *Arkiv. Kemi.* **1**, 463–840.

Bradley, C. J. & Cracknell, A. P. (1972). *The Mathematical Theory of Symmetry in Solids.* Oxford: Clarendon Press.

Brese, N. E. & O'Keeffe, M. (1991). *Acta Cryst.* B**47**, 192–197.

Brown, I. D. (1978). *Chem. Soc. Rev.* **7**, 359–376.

Castro, A., Millan, P., Enjalbert, R., Snoeck, E. & Galy, J. (1994). *Mat. Res. Bull.* **29**, 871–879.

Coppens, P. & Hamilton, W. C. (1970). *Acta Cryst.* A**26**, 71–83.

Diehl, R., Brandt, G. & Salje, E. (1978). *Acta Cryst.* B**34**, 1105–1111.

Kunz, M. & Brown, I. D. (1995). *J. Solid State Chem.* **115**, 395–406.

Loopstra, B. O. & Boldrini, P. (1966). *Acta Cryst.* **21**, 158–162.

Palmer, D. C. (1994). *CrystalMaker.* Lynxvale Ltd, Cambridge.

Rae, A. D. (1987). *Acta Cryst.* A**43**, C-288.

Rae, A. D. (1992). *RAELS*92. *A Comprehensive Constrained Least-Squares Refinement Program.* Australian National University, Australia.

Rae, A. D., Thompson, J. G. & Withers, R. L. (1991). *Acta Cryst.* B**47**, 870–881.

Rae, A. D., Thompson, J. G. & Withers, R. L. (1992). *Acta Cryst.* B**48**, 418–428.

Salje, E. (1977). *Acta Cryst.* B**33**, 574–577.

Thompson, J. G., Rae, A. D., Withers, R. L. & Craig, D. C. (1991). *Acta Cryst.* B**47**, 174–180.

Withers, R. L., Thompson, J. G. & Rae, A. D. (1991). *J. Solid State Chem.* **94**, 404–417.